

**Experimental and Modeling Studies of the Methane Steam Reforming Reaction at  
High Pressure in a Ceramic Membrane Reactor**

Pelin Hacarlioglu

Dissertation submitted to the faculty of the Virginia Polytechnic Institute and State  
University in partial fulfillment of the requirements for the degree of

Doctor of Philosophy

In

Chemical Engineering

S. Ted Oyama, Committee Chair

David F. Cox

Eva Marand

Gerard V. Gibbs

November 12, 2007

Blacksburg, Virginia

Keywords: silica-alumina membrane, hydrogen, steam reforming of methane, one-  
dimensional model, two-dimensional model

Experimental and Modeling Studies of the Methane Steam Reforming Reaction at High Pressure in a Ceramic Membrane Reactor

Pelin Hacarlioglu

**ABSTRACT**

This dissertation describes the preparation of a novel inorganic membrane for hydrogen permeation and its application in a membrane reactor for the study of the methane steam reforming reaction. The investigations include both experimental studies of the membrane permeation mechanism and theoretical modeling of mass transfer through the membrane and simulation of the membrane reactor with 1-D and 2-D models.

A hydrothermally stable and hydrogen selective membrane composed of silica and alumina was successfully prepared on a macroporous alumina support by chemical vapor deposition in an inert atmosphere at high temperature. Before the deposition of the silica-alumina composite, multiple graded layers of alumina were coated on the alumina support with a mean pore size of 100 nm by the sequential application of three boehmite sols with gradually decreasing sol particle sizes of 630, 200 and 40 nm, respectively. The resulting supported composite alumina-silica membrane had high permeability for hydrogen in the order of  $10^{-7}$  mol m<sup>-2</sup> s<sup>-1</sup> Pa<sup>-1</sup> at 873 K with a H<sub>2</sub>/CH<sub>4</sub> selectivity of 940 and exhibited much higher stability to water vapor at the high temperature of 873 K. In addition, the same unusual permeance order of He > H<sub>2</sub> > Ne previously observed for the pure silica membrane

was also observed for the alumina-silica membrane, indicating that the silica structure did not change much after introduction of the alumina. The permeation of hydrogen and helium through vitreous glass and silica membranes was modeled using ab initio density functional calculations. Comparison of the calculated activation energies to those reported for vitreous glass (20–40 kJ mol<sup>-1</sup>) indicated the presence of 5- and 6-membered siloxane rings, consistent with the accepted structure of glass as a disordered form of  $\beta$ -cristobalite.

The experimental studies of the steam reforming of methane were examined at various temperatures (773-923 K) and pressures (1-20 atm) with a commercial Ni/MgAl<sub>2</sub>O<sub>4</sub> catalyst in a hydrogen selective silica-alumina membrane reactor and compared with a packed bed reactor. One-dimensional and two-dimensional modeling of the membrane reactor and the packed bed reactor were performed at the same conditions and their performances were compared with the values obtained in the experimental study. Improved methane conversions and hydrogen yields were obtained in the membrane reactor compared to the packed bed reactor at all temperatures and pressures. From the two modeling studies, it was also found out that the two-dimensional model performed better in the membrane reactor case especially at higher pressures.

## ACKNOWLEDGEMENTS

I would first like to express my gratitude to my advisor, Dr. S. Ted Oyama for his guidance and support during my Ph.D. studies. During my tenure his influence was critical to my development as a research scientist, and I thank him for challenging me to get to this point and encouraging me to continue with my studies.

I would like to thank my other committee members, Dr. Cox, Dr. Marand for their support throughout my research. I would like to express additional thanks to my final committee member, Dr. Gibbs for his continuous help and guidance with my project involving Gaussian calculations.

I would like to thank each group member, past and present that I have worked in the Environmental Catalysis and Nanomaterials Laboratory for their help, and most importantly for their friendship. Current members include Dmitri Iarikov, Haiyan Zhao, Travis Gott and Jason Gaudet and previous group members include Doohwan Lee, Yan Xi, Yongkul Lee, Corey Reed, Juan Bravo, Yuying Shu, Ben Cormier. I especially want to thank Doohwan Lee for making my first steps much easier in this laboratory. Additionally, I want to thank Yungfeng Gu for his influence as a disciplined researcher on me and his guidance during our research projects. Finally I want to thank Hankwon Lim for valuable discussions on our research area and making this research fun for me.

I would also like to thank all the staff in the Chemical Engineering Department at Virginia Tech for their help and specifically to Chris Moore, Riley Chan and Michael Vaught for making our lives easier.

Finally, I want to thank my mom for her encouragement, endless support and patience in every step of my life and I wish that she would have seen its completion. I would like to show my sincerest gratitude to my father for his endless guidance, support and friendship throughout this process. I'm very fortunate to have parents like you and I'm indebted to you for making me a better person and preparing me well equipped for the world ahead.

## TABLE OF CONTENTS

<b>Chapter 1. Introduction .....</b>	<b>1</b>
1.1. Literature Review .....	2
1.1.1. Hydrogen selective silica membranes .....	2
1.1.2. Permeation mechanism through dense silica membranes .....	6
1.1.3. Membrane reactor studies of the methane steam reforming reaction .....	9
1.1.4. Modeling studies of membrane reactors.....	10
1.2. Overview of the present work .....	11
References .....	14
<b>Chapter 2. Hydrothermally-Stable Alumina-Silica Composite Membranes for Hydrogen Separation .....</b>	<b>19</b>
2.1. Introduction .....	19
2.2. Experimental .....	19
2.2.1. Preparation of boehmite sols .....	20
2.2.2. Preparation of intermediate $\gamma$ -alumina multilayer .....	21
2.2.3. Preparation of silica-alumina composite membranes .....	22
2.2.4. Characterization .....	24
2.3. Results and discussion .....	27
2.3.1. Morphology and structure of the composite membranes .....	27
2.3.2. Gas permeation properties of composite membranes .....	29

2.3.3. Permeation mechanism through alumina-silica composite membranes .....	34
2.3.4. Hydrothermal stability of composite membranes .....	39
2.4. Conclusions .....	42
References .....	44
<b>Chapter 3. Activation Energies for Permeation of He and H<sub>2</sub> through Silica Membranes: An Ab Initio Calculation Study .....</b>	<b>45</b>
3.1. Introduction .....	45
3.2. Methodology of the activation energy calculation .....	45
3.3. Previous Studies .....	47
3.4. Results and Discussion .....	49
3.5. Conclusions .....	58
References .....	59
<b>Chapter 4. Studies of the methane steam reforming reaction at high pressure in a ceramic membrane reactor .....</b>	<b>61</b>
4.1. Introduction .....	61
4.2. Experimental .....	62
4.2.1. Catalyst preparation and characterization .....	62
4.2.2. Preparation of hydrogen selective silica-alumina membranes	63
4.2.3. Steam reforming of methane with a membrane reactor .....	63
4.3. Results and Discussion .....	67
4.3.1. Catalyst properties and membrane performances .....	67

4.3.2. Effect of temperature on the performances of the MR and the PBR .....	68
4.3.2. Effect of pressure on the performances of the MR and the PBR .....	71
4.4. Conclusions .....	80
References .....	82
<b>Chapter 5. Modeling studies of the methane steam reforming reaction at high pressure in a ceramic membrane reactor.....</b>	<b>83</b>
5.1. Introduction .....	83
5.2. Experimental .....	84
5.2.1. Preparation of Ni/MgAl <sub>2</sub> O <sub>4</sub> catalysts .....	84
5.2.2. Hydrogen selective silica-based membranes.....	84
5.2.3. Steam reforming of methane in a membrane reactor .....	85
5.2.4. Modeling of steam reforming of methane in a membrane reactor	86
5.3. Results and Discussion .....	94
5.3.1. Comparison of experimental and modeling studies on the performances of the MR and the PBR.....	94
5.3.2. Isothermal two-dimensional model predictions .....	99
5.4. Conclusions .....	104
References .....	105
<b>Chapter 6. Conclusions .....</b>	<b>106</b>
<b>Chapter 7. Future Work .....</b>	<b>109</b>
7.1. Silica Composite Membranes .....	109



7.2. Modeling of membrane reactors .....	111
References .....	112
<b>Vita .....</b>	<b>113</b>

## LIST OF FIGURES

Figure 1.1 Solubility Site in $\beta$ -Cristobalite .....	8
Figure 2.1. Schematic of dual-element CVD apparatus used in the deposition of the alumina-silica composite layer.....	23
Figure 2.2. Scanning electron micrographs of fractured sections of graded $\gamma$ - alumina multilayer substrate and composite alumina-silica membrane	28
Figure 2.3. Changes of gas permeance and selectivity with deposition time of the alumina-silica composite membrane .....	30
Figure 2.4. Changes of gas permeance and selectivity on the alumina-silica composite membrane .....	31
Figure 2.5. Permeation properties of the alumina-silica composite membranes prepared with the use of different molar ratio of ATSB/TEOS in the range of 0.02-0.12 .....	32
Figure 2.6. Permeation properties of the alumina-silica composite membranes prepared with different TEOS concentration .....	33
Figure 2.7. Permeance of gases with different molecule size through the composite membrane .....	35
Figure 2.8. Permeance of He, H <sub>2</sub> , and Ne at different temperature through the composite membrane .....	36
Figure 2.9. Changes in H <sub>2</sub> permeance through the pure silica and composite alumina-silica membranes prepared using different molar ratios of ATSB/TEOS during the exposure to 16 mol% water vapor for 130 h .	41

Figure 2.10. Long-term hydrothermal stability between the pure silica membrane and the composite membrane .....	41
Figure 3.1 Contour plot of the diffusion saddle point of H <sub>2</sub> through 6-membered silica ring .....	47
Figure 3.2 Ball and stick model of the geometry optimized single 4-, 5-, 6-, 7-, and 8- membered silica ring clusters .....	51
Figure 3.3 Evolution of activation energy for diffusion of He and H <sub>2</sub> as a function of distance between diffusing species and the center of the silica ring clusters .....	53
Figure 3.4 Activation energy of diffusion with respect to the distance to oxygen atoms .....	57
Figure 4.1. Schematic diagram of the reactor system .....	66
Figure 4.2. Flux of hydrogen through the silica-based membrane versus pressure .	68
Figure 4.3 a) Fractional conversion of CH <sub>4</sub> in the PBR and the MR at atmospheric pressure, b) Utilization of CH <sub>4</sub> and H <sub>2</sub> O in the PBR and the MR at atmospheric pressure, c) Yield of H <sub>2</sub> , CO and CO <sub>2</sub> in the PBR and the MR at atmospheric pressure .....	70
Figure 4.4 a) Fractional conversion of CH <sub>4</sub> in the PBR and the MR at 873 K, b) Enhancement in the CH <sub>4</sub> conversion in the PBR and the MR at 873 K, c) Utilization of CH <sub>4</sub> and H <sub>2</sub> O in the PBR and the MR at 873 K, d) Yield of H <sub>2</sub> , CO and CO <sub>2</sub> in the PBR and the MR at 873 K .....	73

Figure 4.5 a) Fractional conversion of CH <sub>4</sub> in the PBR and the MR at 923 K,	
b) Enhancement in the CH <sub>4</sub> conversion in the PBR and the MR at 923 K, c)	
Utilization of CH <sub>4</sub> and H <sub>2</sub> O in the PBR and the MR at 923 K,	
d) Yield of H <sub>2</sub> , CO and CO <sub>2</sub> in the PBR and the MR at 923 K .....	75
Figure 5.1. Schematic reaction system model for simulations .....	89
Figure 5.2. a) Fractional conversion of CH <sub>4</sub> in the PBR and the MR at 873 K,	
b) Fractional conversion of CH <sub>4</sub> in the PBR and the MR at 923 K .....	95
Figure 5.3. a) Consumption rates of CH <sub>4</sub> and H <sub>2</sub> O in the PBR and the MR at 873 K,	
b) Consumption rates of CH <sub>4</sub> and H <sub>2</sub> O in the PBR and the MR at 923 K ..	97
Figure 5.4. a) Yields of H <sub>2</sub> , CO and CO <sub>2</sub> in the PBR and the MR at 873 K,	
b) Yields of H <sub>2</sub> , CO and CO <sub>2</sub> in the PBR and the MR at 923 K .....	98
Figure 5.5. a) Radial concentration profiles of hydrogen flow at 873 K,	
b) Radial concentration profiles of hydrogen flow at 923 K .....	100
Figure 5.6. a) Radial and axial concentration profiles of hydrogen at 873 K and 1 atm,	
b) Radial and axial concentration profiles of hydrogen at 873 K and 10 atm,	
c) Radial and axial concentration profiles of hydrogen at 873 K and 20 atm	102
Figure 5.7. a) Radial and axial concentration profiles of hydrogen at 923 K and 1 atm,	
b) Radial and axial concentration profiles of hydrogen at 923 K and 10 atm,	
c) Radial and axial concentration profiles of hydrogen at 923 K and 20 atm	103

## LIST OF TABLES

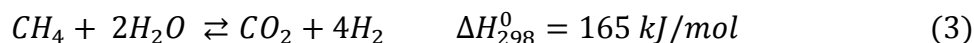
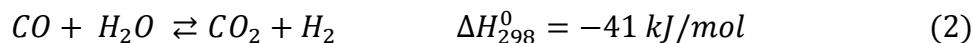
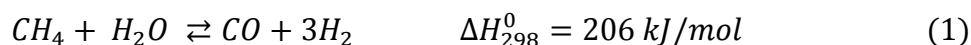
Table 2.1.. Synthesis Parameters of Boehmite Sols with Different Particle Size ...	21
Table 2.2. CVD Process parameters for the preparation of alumina-silica Membranes .....	25
Table 2.3. Effect of substrate on permeation properties of the alumina-silica membranes .....	34
Table 2.4. Calculated parameters for alumina-silica composite membrane .....	38
Table 2.5.. Parameters for Pure Silica and Alumina-Silica Membranes and Silica Glass .....	39
Table 3.1. Bond angle, bond length, and total energy of the silica ring clusters ....	52
Table 3.2. Distances in the planar silica rings and activation energy of diffusion for He and H <sub>2</sub> .....	54
Table 3.3. Bond angle, bond length, and total energy of the silica ring clusters when the gas species are located at the center of the rings .....	55
Table 3.4. Percentage dilations of the silica clusters when gas species are located at the center of the rings .....	56
Table 4.1. Inlet flows of reactants .....	64
Table 4.2. Performance of methane steam reforming processes with membrane reactors .....	78
Table 5.1. Inlet flow rates of the reactants .....	85
Table 5.2. Reaction rates and equilibrium constants for MSR and WGS reactions	87
Table 5.3. Adsorption constants .....	88

Table 5.4. Model equations for the one-dimensional model .....	90
Table 5.5. Model equations for the two-dimensional model .....	91
Table 5.6. Dimensionless quantities and dimensionless model equations .....	92
Table 5.7. Binary and effective diffusivities estimations .....	93
Table 7.1. Composition specifications for natural gas for delivery to the U.S. National Pipeline Grid .....	110

## CHAPTER 1

### INTRODUCTION

Hydrogen is envisioned to be one of the dominant energy carriers of a sustainable energy supply system of the future. At present, natural gas is one of the most viable sources for hydrogen production because of its abundant supply and its relatively low cost. The steam reforming process is currently used commercially to produce hydrogen and synthesis gas (a mixture of H<sub>2</sub> and CO) from natural gas. The catalytic reforming of methane assisted by oxygen (autothermal reforming) is also attractive and is receiving increasing attention [1, 2, 3, 4]. On the other hand, the reforming with carbon dioxide (dry reforming) [5, 6, 7, 8, 9] has been shown [10] to have no chance of commercialization because at high pressure the hydrogen produced is converted to water by the reverse water-gas shift reaction. The methane steam reforming (MSR) involves two reversible reactions:



The two reforming reactions (1,3) are highly endothermic and require high temperatures to obtain high hydrogen productivity. On the other hand, the water-gas shift reaction (2) (WGS) is slightly exothermic and is favored at low temperatures. The

commercial process has two stages; the first carried out at high temperature in a multi tube reactor with a nickel-based catalyst for the reforming reaction and the second at lower temperature for the water-gas shift reactor to enhance CO conversion. This is followed by a pressure-swing adsorption (PSA) system or a cryogenic distillation system to purify the hydrogen [11]. Although an industrial reformer is operated at a pressure range of 8 to 35 bar and a temperature range of 1073-1273 K, the equilibrium-limited process can attain only a methane conversion of 80%. Application of membrane reactors offer a possible way to overcome this limitation by selectively removing hydrogen from the system resulting in higher conversion of methane at a lower temperature, and many membrane reactor studies of MSR have been carried out, but at low pressures.

## **1.1. Literature Review**

### **1.1.1. Hydrogen selective silica membranes**

Silica membranes prepared by chemical vapor deposition (CVD) or sol-gel methods on mesoporous supports are effective for selective hydrogen permeation [12, 13, 14, 15, 16]. However, it is known that hydrogen-selective silica materials are not thermally stable at high temperatures, especially in the presence of water vapor. Most researchers have reported a loss of permeability of silica membranes (as much as 50% or greater in the first 12 h) on exposure to moisture at high temperature. Sea et al. found that the hydrogen permeance of a silica membrane deposited on mesoporous  $\gamma$ -alumina substrates decreased by 90% from  $3.5 \times 10^{-7}$  to  $4.0 \times 10^{-8}$  mol m<sup>-2</sup> s<sup>-1</sup> Pa<sup>-1</sup> after exposure



to 50 mol% water vapor at 400 °C for 100 h [17]. Wu et al. reported a decrease of 62% and 70% in the permeances of He and N<sub>2</sub> for a CVD-deposited silica membrane treated at 600 °C under a N<sub>2</sub> flow containing 20 mol% water vapor [18]. This is because the porous silica (SiO<sub>2</sub>) easily undergoes densification upon exposure to water vapor at elevated temperatures. The densification involves restructuring of the silica by the formation of Si-O-Si bonds from silanol groups (Si-OH) catalyzed by water, leading to the shrinkage of pores [19].

Much effort has been expended on the improvement of the stability of silica membranes. One approach is to make hydrophobic silica membranes prepared by the incorporation of methyl groups in the silica microstructure [20]. Another approach actually involves keeping coated membranes in humid air for a few days and calcining them in steam [21]. Recently, Nomura et al. reported a silica membrane with improved steam stability prepared by counter diffusion CVD of tetramethylorthosilicate and O<sub>2</sub> from opposite sides of the support [22, 23]. The membrane had permeance in the range of  $2\text{-}7 \times 10^{-8} \text{ mol m}^{-2}\text{s}^{-1}\text{Pa}^{-1}$  and a H<sub>2</sub>/N<sub>2</sub> permeance ratio of over 800 for 21 h at 773 K. Also recently, Kanezashi and Asaeda reported Ni-doped silica membranes that showed good steam tolerance with a H<sub>2</sub> permeance of  $2.0 \times 10^{-7} \text{ mol m}^{-2}\text{s}^{-1}\text{Pa}^{-1}$  and H<sub>2</sub>/N<sub>2</sub> selectivity of 400 after 140 h in steam at 773 K [24].

Composite membranes prepared by sol-gel methods composed of silica with other inorganic oxides such as alumina (Al<sub>2</sub>O<sub>3</sub>), titania (TiO<sub>2</sub>) and zirconia (ZrO<sub>2</sub>) have been reported to improve the stability of silica membranes for use under humid atmospheres at

high temperature. Fotou et al. [25] introduced these oxides and MgO into the membranes by doping the starting silica sol with controlled amounts of the corresponding nitrate salts. They found that the mean pore size did not change much from 0.6 nm to 0.7 nm, but the hydrothermal stability was improved after doping with 3% alumina. A heat treatment in 50 mol% steam/air at 600 °C for 30 h resulted in 64% reduction in the surface area and a loss of 86% micropore volume for the unsupported 3% alumina-doped silica membrane, compared to 85% and 94%, respectively for a pure silica membrane. They also reported that 6% alumina-doped and magnesia-doped silica membranes were not improved, since the surface area was substantially reduced compared with the pure silica. These data were consistent with the permeation properties of the sol-gel derived SiO<sub>2</sub>-10 mol%Al<sub>2</sub>O<sub>3</sub> and SiO<sub>2</sub>-10 mol%TiO<sub>2</sub> on gamma-alumina membranes reported by Hekkink et al. [26]. The H<sub>2</sub> permeances at 298 K were  $7 \times 10^{-7}$ ,  $2.2 \times 10^{-7}$  and  $6 \times 10^{-8}$  mol m<sup>-2</sup> s<sup>-1</sup> Pa<sup>-1</sup> for pure SiO<sub>2</sub>, 10 mol% TiO<sub>2</sub>-SiO<sub>2</sub> and 10 mol% Al<sub>2</sub>O<sub>3</sub>-SiO<sub>2</sub> membranes, respectively. Yoshida et al. investigated the hydrothermal stability of sol-gel derived silica-zirconia membranes with a content of zirconia of 10-50 mol% [27]. After a 20 h-exposure to a high temperature of 773 K and steam at levels of 13-33 mol%, the 10 mol% ZrO<sub>2</sub>-SiO<sub>2</sub> membrane still suffered a decrease of H<sub>2</sub> permeance of 70 % to  $8.9 \times 10^{-8}$  mol m<sup>-2</sup> s<sup>-1</sup> Pa<sup>-1</sup>, but with an increased selectivity of H<sub>2</sub> to N<sub>2</sub> of 190, while the 50 mol% ZrO<sub>2</sub>-SiO<sub>2</sub> membrane did not show any change in the H<sub>2</sub> permeance but a constant H<sub>2</sub>/N<sub>2</sub> selectivity of 4.0.

The composite membranes prepared by the chemical vapor deposition technique generally have a better selectivity but a lower permeance in comparison to those obtained

with the sol-gel method. Nam et al. made TiO<sub>2</sub>-SiO<sub>2</sub> membranes at 873 K on porous Vycor glass with a mean pore diameter of 4 nm by hydrolysis of tetraisopropyl titanate (TIPT) and tetraethylorthosilicate (TEOS) at atmospheric pressure [28]. A wide range (0.1-7.0) of molar ratios of TIPT/TEOS was used in their work. The obtained composite membranes showed high hydrogen selectivities of around 500 but with a low permeance of  $2 \times 10^{-8}$  mol m<sup>-2</sup> s<sup>-1</sup> Pa<sup>-1</sup> at 873 K. The low permeance was the result of the intrinsic low permeability of Vycor glass. No stability data was reported.

To obtain ceramic membranes with both high selectivity and permeance, some researchers have used mesoporous (pore diameter of 2-50 nm) or macroporous (pore diameter larger than 50 nm) supports to decrease the resistance of the supports. Using an intermediate mesoporous gamma-alumina layer, Yan et al. placed the silica in the pores of the support by CVD and obtained a H<sub>2</sub> permeance of  $1.8 \times 10^{-7}$  mol m<sup>-2</sup> s<sup>-1</sup> Pa<sup>-1</sup> but a selectivity of H<sub>2</sub> to N<sub>2</sub> of only 26 at 873 K [14]. Lee et al. made membranes with the silica layer on the outer surface of a mesoporous alumina support and obtained a H<sub>2</sub> permeance of  $1.2 \times 10^{-7}$  mol m<sup>-2</sup> s<sup>-1</sup> Pa<sup>-1</sup> and a selectivity of H<sub>2</sub> to CH<sub>4</sub> of 2800 at 873 K [29].

Recently, we have successfully prepared a  $\gamma$ -alumina multilayer membrane with a graded structure by sequentially placing boehmite sols of different particle sizes on a macroporous alumina support. The multilayer graded structure had a thickness of around 1  $\mu$ m and was substantially defect-free. After deposition of a thin silica layer by CVD, the resulting novel silica-on-alumina membranes had excellent permeability of  $5 \times 10^{-7}$

$\text{mol m}^{-2} \text{s}^{-1} \text{Pa}^{-1}$  and good selectivity for hydrogen over  $\text{CO}_2$ , CO and  $\text{CH}_4$  of 1500-5900 at 873 K.

### **1.1.2. Permeation mechanism through dense silica membranes**

There has been much interest in silica-based hydrogen-selective membranes since the work of Okubo and Inoue [12] and Gavalas and collaborators [13], and much progress has been reported recently [30,31,32,33,34]. Gas permeation properties for microporous inorganic membranes, including zeolite membranes have been described by Knudsen [35], surface [36], and activated-type-Knudsen diffusion mechanisms [37,38,39]. However, until recently detailed studies on the mechanism of gas transport through dense silica membranes have not been reported [40]. It was found in these membranes that the order of permeability of small gas molecules was  $\text{He} > \text{H}_2 > \text{Ne}$ , which is unusual because the order does not follow the mass or size of the diffusing species. The order cannot be rationalized by the existing mechanisms, but was successfully explained using a statistical mechanical treatment, in which the diffusion of the gas molecules was described as involving jumps between adjacent solubility sites in the dense silica structure.

The structure of the silica membranes obtained by high temperature CVD of  $\text{SiO}_2$  on porous supports can be considered to be similar to that of vitreous silica glass, which can be visualized as a disordered form of  $\beta$ -cristobalite [41]. For example, the radial distribution function for first neighbors is the same for amorphous silica glass and  $\beta$ -

crystoballite [42]. The structure of  $\beta$ -cristobalite is built up of 6-membered rings, but in the process of glass formation through fusion, bonds break and reform to create a random network containing 5-, 6-, 7-, and 8-membered silicate rings. The structure forms solubility sites of approximately 0.3 nm in diameter (the solubility site of  $\beta$ -cristobalite is shown in Figure 1) [43]. Basically, the restricted size of the interstitial solubility sites in the dense silica membranes allows accommodation of only small species (He = 0.26 nm, Ne = 0.275 nm, H<sub>2</sub> = 0.289 nm [44]) that are smaller than the size of the solubility sites, while prohibiting sorption of large gas molecules (CO<sub>2</sub> = 0.33 nm, CO = 0.376 nm, CH<sub>4</sub> = 0.38 nm [44]). It was concluded that the unusual permeance order resulted from differences in mobility of the diffusing species and differences in the number of solubility sites available for each diffusing species in the silica membrane. It was also found that the activation energies for permeation through the membranes were smaller (He = 8.0 kJ mol<sup>-1</sup>, H<sub>2</sub> = 14.8 kJ mol<sup>-1</sup>, Ne = 16.6 kJ mol<sup>-1</sup>) than those for vitreous glass reported in the literature (H<sub>2</sub> = 37.2 – 38.8 kJ mol<sup>-1</sup> [45, 46], He = 17.8 – 21.3 kJ mol<sup>-1</sup> [47, 48, 49], Ne = 33.8 – 39.5 kJ mol<sup>-1</sup> [50, 51]). These results indicated that the interstitial structure of the dense silica membranes allowed easier passage of the small gas molecules compared to the vitreous silica.

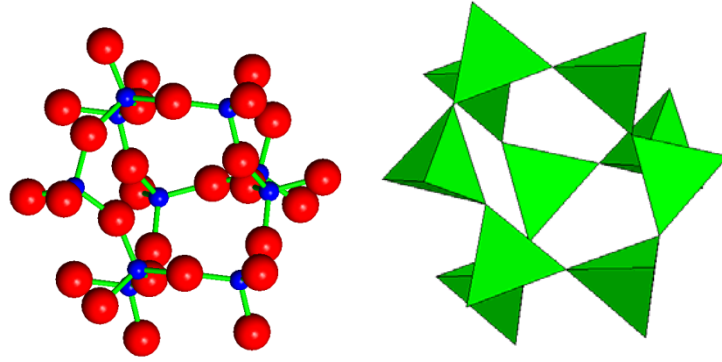


**Figure 1.1** Solubility Site in  $\beta$ -Cristobalite a) Ball-and-stick model of the solubility site. Large spheres = oxygen, small spheres = silicon b) Polyhedral representation of the same site. Each vertex is an oxygen atom. There are four 6-membered rings (doorways) which are tetrahedrally oriented.

The activation energy of transport through the silica membranes was obtained empirically by fitting permeation data at different temperatures to an expression derived for jumps between solubility sites.

$$Q = \frac{1}{6L} \left( \frac{d^2}{h} \right) \left( \frac{h^2}{2\pi mkT} \right)^{3/2} \left( \frac{\sigma h^2}{8\pi^2 IkT} \right)^\alpha \frac{(N_s/N_A)}{(e^{hv^*/2kT} - e^{-hv^*/2kT})^2} e^{-\Delta E_K/RT} \quad (1.1)$$

In this equation  $Q$  is the permeance of a monatomic gas ( $\text{mol/m}^2 \text{ s Pa}$ ),  $L$  is the thickness of the membrane (m),  $d$  is the jump distance (m),  $m$  is the mass of the species (kg),  $h$  is Planck's constant (J s),  $k$  is Boltzmann's constant (J/K),  $v^*$  is the vibrational frequency of the species in the passageways between the sorption sites ( $\text{s}^{-1}$ ),  $T$  is temperature (K),  $N_s$  is the number of solubility sites available per  $\text{m}^3$  of silica volume ( $\text{m}^{-3}$ )

<sup>3</sup>),  $N_A$  is Avogadro's number ( $\text{mol}^{-1}$ ),  $R$  is the gas constant ( $\text{kJ/mol K}$ ),  $\Delta E_K$  is the activation energy for hopping between sorption sites ( $\text{kJ/mol}$ ),  $I$  is the moment of inertia ( $\text{kg m}^2$ ) and  $\sigma$  is the symmetry number of the permeating species, with  $\sigma = 2$  in the case of hydrogen. The exponent,  $\alpha$ , accounts for incomplete loss of rotation, with  $\alpha = 0$  for a non-rotating transition state.

### **1.1.3. Membrane reactor studies of the methane steam reforming reaction**

Membrane separation among many other separation technologies has recently drawn attention because of its ability to remove hydrogen from the reaction systems. In addition to the simplified downstream separation, recovery and enhanced selectivity, combining the reaction and separation steps in one unit offers savings in energy consumption and extends the life of reactor materials and catalysts. According to the Le Chatelier-Braun's law, the continuous withdrawal of a product, in this case hydrogen, from the system shifts the equilibrium of the reforming reaction to the product side and enhances yields. Many membrane reactor studies of MSR have been carried out, but at low pressures [62, 63, 64, 65, 68, 52, 53, 54, 55, 56, 57, 58]. Recent improvements in inorganic membranes allow the use of high temperature and pressure conditions. A key point is to use optimum reaction conditions in which the hydrogen removal rate is comparable to the production rate.

Typical membranes reported in the literature are dense palladium membranes [59, 60, 61] or silver-palladium membranes [56, 57]. These membranes show extremely high

selectivity over other gases due to the selective dissolution of hydrogen atoms into the metal matrix. On the other hand, their high cost and problems of carbon deposition and poisoning by impurities such as sulfur and chlorine, or even carbon monoxide, are drawbacks in the application of these types of membranes. Recently, a number of studies have reported the use of alumina membranes [56] and microporous silica membranes [57] for the steam reforming of methane. Although these types of membranes are very sensitive to water vapor, successful results have been obtained in several cases. The future of membrane reactors in hydrogen production from the reforming of methane lies in the development of new membranes and in the optimization of the operating conditions (temperature, pressure, flow rates).

#### **1.1.4. Modeling studies of membrane reactors**

The modeling of catalytic membrane reactors has been the subject of considerable research. Much work has been carried out with one-dimensional (1-D) models where only axial concentration changes are calculated, because of the simplicity of the methods [56, 57, 58, 60, 62, 63, 64, 65, 66, 67, 68, 69, 70, 71, 72, 73]. More limited work has been done with two-dimensional (2-D) models, where both axial and radial concentration profiles are mapped, because of the need for more elaborate mathematical treatments. The most commonly used numeric tools for 2-D analysis are finite differences [74], orthogonal collocation [65] and in a few cases, finite volume methods [75].



The principal objectives of the modeling of membrane reactors are to simulate their performance in terms of attainable reactant conversions [52], to analyze the effects of differences in the system structures and types of permeable membranes on the reactor characteristics [66], to evaluate the relationship between the differences in the membranes permeation mechanism and the reactor performance [67, 68] and to make predictions about the reactor behavior [71]. In meeting these objectives 2-D analysis, which considers mass transfer in the radial direction, is expected to produce a more precise estimation of the performance characteristics of the membrane reactor. Two-dimensional studies, including temperature profiles, have been performed for the hydrogenation of propane [76] and have given excellent results. Non-ideal flow effects have also been examined successfully by using dispersion coefficients in the modeling of an industrial-scale membrane reactor [77]. Nevertheless, one-dimensional studies have also been effective in describing the behavior of membrane reactors [62, 63, 65, 66].

## **1.2. Overview of the present work**

Chapter 1 summarized background information and the motivation of this work. It describes the inorganic silica-based membranes used in the experimental portion of this work, the theory of permeance through these membranes, the application of density functional theory to calculate activation energies of permeation and theory of 1-D and 2-D simulations to describe reactor performance.

In Chapter 2, the synthesis, characterization and gas permeation properties of alumina-silica composite membranes are presented in detail. The membranes were prepared on a graded mesoporous  $\gamma$ -alumina multilayer supported on macroporous  $\alpha$ -alumina tubes by employing a dual-element CVD technique at high temperature. The permeation properties and hydrothermal stability of the obtained composite membranes are among the best reported so far.

Chapter 3 describes an ab initio method of calculating activation energies which utilizes a simplified model for the structure of the silica membrane. Basically on jumping from site to site the permeating species is considered to pass through a single critical ring opening. A hybrid functional of the density functional theory (DFT) method with a highly accurate basis set is used to optimize ring structures and the gas species.

In Chapter 4, a membrane reactor study of the steam reforming of methane is presented. The studies were conducted at various temperatures (773- 923 K) and pressures (1-20 atm) and the performance of this reactor was compared with a packed-bed reactor operated under the same conditions. The membrane described in Chapter 2 was used in this study. These hydrothermally-stable membranes allowed the application of high temperature and pressure conditions in this work.

Chapter 5 combines experimental results obtained in a membrane reactor with a 1-D and 2-D analysis of the results to develop a criterion for the use of these two types of treatment. The experimental studies of the methane steam reforming were conducted in a membrane reactor and a packed-bed reactor at various temperatures (873K and 923 K)

and pressures (1-20 atm). The studies are conducted at low and high pressure to ensure that the system crosses the boundary that separate the regions requiring 1-D and 2-D analysis. One-dimensional and two-dimensional models were developed based on rate expressions obtained from the literature and were validated by comparison to the experimental results.

## References

---

- [1] Y-S. Seo, A. Shirley, S. T. Kolazkowski, *J. Power Sources*, 108 (2002) 213
- [2] J. A C Dias, J. M. Assaf, *J Power Sources*, 130 (2004) 106
- [3] K. Takehira, T. Shishido, P. Wang, T. Kosaka, K. Tataka, *J. Catal.*, 221 (2004) 43
- [4] M. M. V. M. Souza, M. Schmal, *Appl. Catal. A*, 281 (2005) 19
- [5] J. Munera, S. Irusta, L. Cornaglia, E. Lombardo, *Appl Catal. A*, 245 (2003) 383
- [6] B. S. Liu, C. T. Au, *Catal. Letters*, 77 (2001) 67
- [7] T. Ioannides, X. E. Verykios, *Catal. Letters*, 36 (1996) 165
- [8] A. K. Prabhu, S T. Oyama, *J. Memb. Sci.*, 176 (2000) 233
- [9] T. M. Raybold, M. C. Huff. *AIChE J.*, 48 (2002) 1051
- [10] D. Lee, P. Hacırlıoğlu, S. T. Oyama, *Topics in Catal*, 29 (2004) 45
- [11] H. F. Rase, *Handbook of Commercial Catalysts: Heterogeneous Catalyst*, New York: CRC Press, 2000, 405
- [12] T. Okubo, H. Inoue, *J. Membr. Sci.* 42 (1989) 109-117.
- [13] G.R. Gavalas, C.E. Megiris, S.W. Nam, *Chem. Eng. Sci.* 44 (1989) 1829-1835.
- [14] S. Yan, H. Maeda, K. Kusakabe, S. Morooka, Y. Akiyama, *Ind. Eng. Chem. Res.* 33 (1994) 2096-2101.
- [15] S. Gopalokrishnan, Y. Yoshino, M. Nomura, B. N. Nair, S. Nakao, *J. Membr. Sci.* 297 (2007) 5-9.
- [16] S. Araki, N. Mohri, Y. Yoshimitsu, Y. Miyake, *J. Membr. Sci.* 290 (2007) 138-145.
- [17] B-K. Sea, E. Soewito, M. Watanabe, K. Kusakabe, S. Morooka, S.S. Kim, *Ind. Eng. Chem. Res.* 37 (1998) 2502-2508.

- 
- [18] J.C.S. Wu, H. Sabol, G.W. Smith, D.L. Flowers, P.K.T. Liu, *J. Membr. Sci.* 96 (1994) 275-287
- [19] Iler, *The Chemistry of Silica*, Wiley, New York, 1979
- [20] R.M. de Vos, W.F. Maier, H. Verweij, *J. Membr. Sci.*, 158 (1999) 277-288
- [21] M. Asaeda, M. Kashimoto, *Proc. Fifth Inter. Conf. Inorg. Membr.* p.172, Nagoya, Japan (1998)
- [22] M. Nomura, H. Aida, S. Gopalakrishnan, T. Sugawara, S. Nakao, S. Yamazaki, T. Inada, Y. Iwamoto, *Desalination* 193 (2006) 1-7
- [23] M. Nomura, M. Seshino, H. Aida, K. Nakatani, S. Gopalakrishnan, T. Sugawara, T. Ishikawa, M. Kawamura, S. Nakao, *Ind. Eng. Chem. Res.* 45 (2006) 3950
- [24] M. Kanezashi, M. Asaeda, *J. Membr. Sci.* 271 (2006) 86-93
- [25] G.P. Fotou, Y.S. Lin, S.E. Pratsinis, *J. Mater. Sci.* 30 (1995) 2803-2808
- [26] J.H.A. Hekkink, R.S.A. De Lange, A.A. Ten Hoeve, P.J.A.M. Blankenvoorde, K. Keizer, A.J. Burggraaf, *Key Eng. Mater.* 61&62 (1991) 375-378
- [27] K. Yoshida, Y. Hirano, H. Fujii, T. Tsuru, M. Asaeda, *J. Chem. Eng. Japan*, 34 (2001) 523-530
- [28] S.W. Nam, H.Y. Ha, S.P. Yoon, J. Han, T.H. Lim, I.-H. Oh, S.-A. Hong, *Korean Membr. J.*, 3 (2001) 69-74
- [29] D. Lee, L. Zhang, S. T. Oyama, S. Niu, R.F. Saraf, *J. Membr. Sci.*, 231 (2004) 117-126.
- [30] H. Verweij, Y. S. Lin, J. Dong, *MRS Bull.* 31 (2006) 756
- [31] M. Kanezashi, M. Asaeda, *J. Membr. Sci.* 271 (2006) 86
- [32] S. Araki, N. Mohri, Y. Yoshimitsu, Y. Miyake, *J. Membr. Sci.* 290 (2007) 138

- 
- [33] T. Zivkovic, N.E. Benes, D.H.A. Blank, H.J.M. Bouwmeester, *J. Sol-Gel. Sci. Technol.* 31 (2004) 205
- [34] S. Gopalakrishnan, Y. Yoshino, M. Nomura, B. N. Nair, S.-I. Nakao, *J. Membr. Sci.* 297 (2007) 5
- [35] M. Knudsen, *Ann. Phys.* 28 (1909) 75
- [36] S.-T. Hwang, K. Kammermeyer, *Can. J. Chem. Eng.* 44 (1966) 82
- [37] J. Xiao, J. Wei, *Chem. Eng. Sci.* 47 (5) (1992) 1123
- [38] A.B. Shelekhin, A.G. Dixon, Y.H. Ma, *AIChE Journal* 41 (1) (1995) 58
- [39] A. J. Burggraaf, *J. Membr. Sci.* 155 (1999) 45
- [40] S. T. Oyama, D. Lee, P. Hacırlıoğlu, R. F. Saraf, *J. Membr. Sci.* 244 (2004) 45
- [41] D. Davazoglou, V. Em. Vamvakas *J. Electrochem. Soc.*, 150 (2003) F90
- [42] R. L. Mozzi, B. E. Warren, *J. Appl. Crystallogr.* 2 (1969) 164.
- [43] R. M. Barrer, D. E. W. Vaughan, *Trans. Faraday Soc.* 63 (1967) 2275
- [44] D. W. Breck, *Zeolite Molecular Sieves: Structure, Chemistry and Use*, Wiley, New York, 1974, 636
- [45] R. W. Lee, R. C. Frank, D. E. Swets, *J. Chem. Phys.* 36 (1962) 1062
- [46] R.W. Lee, *J. Chem. Phys.* 38 (1963) 448
- [47] J. E. Shelby, *J. Am. Ceram. Soc.* 55 (2) (1972) 61
- [48] J. E. Shelby, *J. Am. Ceram. Soc.* 54 (2) (1972) 125
- [49] R. W. Lee, R. C. Frank, D. E. Swets, *J. Chem. Phys.* 34 (1961) 17
- [50] J. E. Shelby, *J. Am. Ceram. Soc.* 56 (6) (1973) 340
- [51] W. G. Perkins, D. R. Begeal, *J. Chem. Phys.* 54 (4) (1971) 1683

- 
- [52] G. Barbieri, V. Violante, F. P. Di Maio, A. Criscuoli, E. Drioli, *Ind. Eng. Chem. Res.* 36 (1997) 3369
- [53] E. Kikuchi, *Catal. Today* 56 (2000) 97
- [54] L. Paturzo, A. Basile, *Ind. Eng. Chem. Res.* 41 (2002) 1703
- [55] J. Tong, Y. Matsumura, H. Suda, K. Baraya, *Ind. Eng. Chem. Res.* 44 (2005) 1454
- [56] E. Kikuchi, S. Uemiya, T. Matsuda, *Stud. Surf. Sci. Catal.* 61 (1991) 509
- [57] F. Gallucci, L. Paturzo, A. Fama, A. Basile, *Ind. Eng. Chem. Res.* 43 (2004) 928
- [58] M. Chai, M. Machida, K. Eguchi, H. Arai, *Appl. Catal. A.* 110 (1994) 239
- [59] S. Uemiya, N. Sato, H. Ando, T., Matsuda, E Kikuchi, *Appl. Catal.* 67 (1991) 223
- [60] J. Shu, B. P.A. Grandjean, S. Kaliaguine, *Appl. Catal. A.* 119 (1994) 305
- [61] J. Tong, Y. Matsumura, H. Suda, K. Haraya, *Ind Eng Chem Res*, 44 (2005) 1454
- [62] E. Kikuchi, Y. Nemoto, M. Kajiwara, S. Uemiya, T. Kojima, *Catal. Today* 56 (2000) 75
- [63] G. Marigliano, G. Barbieri, E. Drioli, *Chem. Eng. Process* 42 (2003) 231
- [64] A. Basile, L. Paturzo, F. Lagana, *Catal. Today* 67 (2001) 65
- [65] J. Shu, B. P. A. Grandjean, S. Kaliaguine, *Appl. Catal. A.* 119 (1994) 305
- [66] Y. M. Lin, S. L. Liu, C. H. Chuang, Y. T. Chu, *Catal. Today.* 82 (2003) 127
- [67] W. S. Moon, S. B. Park, *J. Memb. Sci.* 170 (2000) 43
- [68] T. Tsuru, K. Yamaguchi, T. Yoshioka, M. Asaeda, *AIChE J.* 50 (2004) 2794
- [69] W. Jin, X. Gu, S. Li, P. Huang, N. Xu, J. Shi, *Chem. Eng. Sci.* 55 (2000) 2617
- [70] J. C. S. Wu, P. K. T. Liu, *Ind. Eng. Chem. Res.* 31 (1992) 322

- 
- [71] W. Yu, T. Ohmori, T. Yamamoto, A. Endo, M. Nakaiwa, T. Hayakawa, N. Itoh, *Int. J. Hydrogen Energy* 30 (2005) 1071
- [72] J. H. Kim, B. S. Choi, J. Yi, *J. Chem Eng. Jpn.* 32 (1999) 760
- [73] D. L. Hoang, S. H. Chan, O. L. Ding, *Chem. Eng. Res. Des.* 83 (2005) 177
- [74] T. Brinkmann, S. P. Perera, W. J. Thomas, *Chem. Eng. Sci.* 56 (2001) 2047
- [75] K. A. Hoff, J. Poplsteinova, H. A. Jakobsen, O. Falk-Pedersen, O. Juliussen, H. F. Svendsen, *Int. J. Chem. Reactor Eng.* 1 (2003) 1
- [76] K. Hou, R. Hughes, R. Ramos, M. Menendez, J. Sanatamaria, *Chem. Eng. Sci.* 56 (2001) 57
- [77] M. K. Koukou, N. Papayannakos, N. C. Markatos, *Chem Eng. J.* 83 (2001) 95